Comparing DINA code simulations with TCV experimental plasma equilibrium responses

R.R. Khayrutdinov[2], J.B. Lister[1], V.E. Lukash[3], J.P. Wainwright[4]

[1] Centre de Recherches en Physique des Plasmas, Association EURATOM-Confédération Suisse, Ecole Polytechnique Fédérale de Lausanne, 1015 Lausanne, Switzerland
[2] RRC Kurchatov Institute, Moscow, Russia
[3] TRINITI, Troitsk, Russia
[4] Imperial College of Science, Technology and Medicine, Electrical and Electronic Engineering, Prince Consort Road, London SW7 2BY, U.K.

ABSTRACT

The DINA non-linear time dependent simulation code has been validated against an extensive set of plasma equilibrium response experiments carried out on the TCV tokamak. Limited and diverted plasmas are found to be well modelled during the plasma current flat top. In some simulations the application of the PF coil voltage stimulation pulse sufficiently changed the plasma equilibrium that the vertical position feedback control loop became unstable. This behaviour was also found in the experimental work, and cannot be reproduced using linear time-independent models. A single null diverted plasma discharge was also simulated from start-up to shut-down and the results were found to accurately reproduce their experimental equivalents. The most significant difference noted was the penetration time of the poloidal flux, leading to a delayed onset of sawtoothing in the DINA simulation. The complete set of frequency stimulation experiments used to measure the open loop tokamak plasma equilibrium response was also simulated using DINA and the results were analysed in an identical fashion to the experimental data. The frequency response of the DINA simulations agrees with the experimental results. Comparisons with linear models are also discussed to identify areas of good and only occasionally less good agreement.

1 INTRODUCTION

Considerable attention is being focused on the design of plasma position, current and shape controllers for the next generation of tokamak reactor designs like ITER-FEAT. The development of a new control algorithm for a new plasma configuration will require extensive numerical analysis prior to experimental tests to optimise expensive experimental time. A validated tokamak plasma simulation tool is therefore a requirement to test any proposed plasma controller design. The first requirement of such a tool must be its ability to model experimental plasma evolution to sufficient accuracy. Previous work has focused on linear models and considerable success has been obtained in the past in modelling the flat top plasma current phase of TCV

(Tokamak à Configuration Variable) discharges using the RZIP and CREATE-L models [1, 2, 3].

The major assumptions made when creating a dynamic linear model of a tokamak are that the equilibrium is time-invariant and the disturbances have small amplitude. The behaviour of the plasma current is modelled in different ways but usually involves assuming that some aspect of the plasma current profile is constant while the total plasma current can vary. With the RZIP model the plasma current profile shape is assumed to be constant, while the CREATE-L model assumes that the functions describing the current profile are fixed but that the shape coefficients can change in order to conserve various quantities. When comparing experimental data with the linear models we might therefore expect to see signs of ***:***

- large amplitude non-linearities;
- non-time-invariant non-linearities;
- disagreement with linearised models due to modifications of the current profile, such as those due to current penetration;
- disagreement with linearised models if the equilibrium varies significantly during the pulsed stimulation, for instance the poloidal beta or vacuum field configuration might change.

The DINA code will model such effects and is therefore a suitable candidate for full discharge modelling [4].

TCV was chosen for an exhaustive test of the DINA plasma equilibrium response due to the existence of the data from plasma equilibrium response experiments already compared with the linear models [1, 2, 3]. TCV has 18 separately powered Poloidal Field (PF) coils outside the vessel and its full control system is described in detail elsewhere [5]. Figure 1 shows a poloidal cross section of TCV, showing the positions of the 8 E-coils on the inboard side of the vacuum vessel, the 8 F-coils on the outboard side of the vessel and the up-down symmetric OH1 and OH2 coils. The separatrix for the diverted discharges discussed in this paper is shown as a solid line in the figure. TCV has extensive and well calibrated diagnostics for evaluating the experimental plasma equilibrium response. For highly unstable plasmas, internal coils can also be used on TCV [6], but this was not the case for the modest growth rate plasmas used in this paper.

The DINA code is a tokamak plasma simulation code comprising a 1.5D axisymmetric, time-dependent, resistive magnetohydrodynamic (MHD) and transport-modelling free boundary equilibrium solver given an externally imposed magnetic field [4]. The axisymmetric Grad-Shafranov equation is solved at each integration time step as the plasma current and conductor currents evolve according to Ohm's law. An "inverse variable" equilibrium calculation for determining the mapping between equilibrium flux co-ordinates and a rectangular grid allows rapid and accurate numerical convergence. A flux surface averaged 1D system of transport equations is self-consistently solved for the following plasma parameters:

- electron temperature;
- ion temperature;
- density of plasma components;
- poloidal magnetic flux.

The plasma is assumed to be massless as well as non-viscous, eliminating processes on the

Alfvén timescale. Using simple transport laws DINA is capable of rapidly calculating the plasma evolution for both normal discharges and disruptive discharge termination. The effects of eddy currents in the surrounding conductors such as the vacuum vessel are included in the circuit equations for the toroidally symmetric passive structure currents. Halo-current and runaway electron models, neutral beam and radio-frequency heating or current drive, α-particle heating, the pressure driven bootstrap current, as well as fuelling by pellet injection have all been included in the DINA code for specific applications. Pre-programmed control parameters are introduced into an active feedback control system model. In the past, DINA has mainly been used in two areas: plasma control simulations and disruption analyses. Previous DINA simulations for plasma control scenarios have been carried out for DIII-D [7, 8] and ITER [9] tokamaks. Disruption phenomena have been studied in DIII-D [10, 7], JT-60 [11] and ITER [12] tokamaks.

For the TCV equilibrium response simulations described in this paper, not all the cited features of the DINA code were used and the following simplifications were made:

- there is no particle or energy transport ;
- electron temperature and Z_{eff} profiles are prescribed and chosen to make the values of internal inductance (l_i) and plasma resistance approximate the experimental data;
- poloidal magnetic flux transport assumes neo-classical plasma resistivity;
- the plasma current density profile, fitted PF coil and vacuum vessel currents for the initial equilibrium are taken from results of the LIUQE inverse equilibrium calculations [13];
- sawtooth oscillations are assumed to start when the safety factor on axis $q(0) < 0.9$.

These simplifications remove any problems associated with accurately modelling transport, but lead to the requirement that the profiles be imposed.

The TCV feedback control system was expressed in discrete time state-space form by the gain matrices Ak, Bk, Ck, Dk as:

$$x_{n+1} = Ak \bullet x_n + Bk \bullet (cp(t_n)-cp_{ref}(t_n))$$
$$U_n = Ck \bullet x_n + Dk \bullet (cp(t_n)-cp_{ref}(t_n)) \qquad (1)$$

where the vector of parameters under feedback control for these experiments (cp) is: P-VERT (current weighted radial position), TRI-IN (current weighted inboard surface straightness), TRI-OUT (current weighted outboard surface straightness), zIp (current weighted vertical position) and Ip (total plasma current). x_n is the state vector at time t_n. The control parameters are estimated using a matrix multiplication on the vector of all the simulated "measurement" data from the DINA code namely the 38 poloidal flux loops, 38 tangential poloidal field probes and the 18 PF coil currents. This is exactly the same as the TCV real time control system. The power supply delay was modelled as 0.3ms for all the TCV shots simulated. Each simulation generated its own consistent power supply control voltages from the errors between the control parameter estimates and the time-dependent control parameter reference signals used on TCV.

The effort required to implement TCV in the DINA code and to get correct closed loop

simulation was modest. The basic electromagnetic properties, the feedback control circuits and the time-dependent control waveforms were imported from the TCV data archive and used as DINA input. After implementing a single test case and making some improvements, detailed in Section 2, the main task was to benchmark the available experimental data from particular TCV control experiments, against the non-linear time dependent DINA code, including the full TCV feedback matrices. Future work will compare the vertical instability growth rate and evolution of the plasma with TCV Vertical Displacment Event experiments [14].

The remainder of the paper is laid out as follows. In Section 2 we present the DINA simulations of TCV experiments with square wave stimulation of the PF coil voltages during the flat top phase of both limited and diverted plasmas and we present a complete scenario simulation. In Section 3 we describe numerical closed loop experiments with multiple sine wave stimulation of the PF coil voltages, as performed on TCV. The analysis is improved, considering the voltages applied directly to the coils rather than the voltage demand signals to the power supplies. The advantage of this modification to our previous approach is discussed. The time domain and frequency domain results show excellent agreement between TCV and the DINA simulations, whereas the linear modelling shows occasional significant differences. The origins of these differences are discussed in Section 4. Section 5 closes the paper with a discussion.

2 COMPARISONS IN THE TIME DOMAIN

2.1 Trial simulations to test the method

Two significant techniques were found to improve the quality of the DINA simulations during initial test runs. Following these adjustments described in this section, all 26 discharges discussed in this paper were simulated successfully at the first attempt, with a single exception due to an obscure numerical condition which was rectified after being encountered. Filtering of the data is also described.

Feedback controller initialisation: The feedback algorithm used for these discharges (PCG [5]) has a high low frequency gain due to the integral gain feedback required to obtain very small asymptotic errors. When starting the simulations, a significant transient was observed before the simulation settled down to reproduce the TCV time traces accurately. We found that this transient was due to two effects. The smaller effect was due to the different equilibrium parametrisation used by the LIUQE inverse equilibrium code and the DINA simulation code, requiring a short transient before the equilibrium relaxes to a self-consistent DINA equilibrium. The dominant effect was due to the simulation of the low frequency gain of the feedback controller. For a linearised simulation, the feedback controller states can be self consistently initialised to zero with the initial errors also set equal to zero. For a non-linear model the feedback control parameters can have, and indeed usually do have, significant control actions at the start of the simulation. If these are not correctly included, the simulation has to start by generating an error in order to set up the feedback controller low frequency response. In our simulations this transient

took about 50msec to die down. After looking at several approaches to this problem we finally settled on requiring that the initial feedback controller states (x_0) should create the initial measured TCV controller outputs (δV), such that:

$$x_0 = Ck^{-1} \bullet \delta V \qquad (2)$$

where the inverse of Ck is performed using a pseudo-inverse technique. This approach gave an important improvement to the start of the simulations, illustrated in Fig.2. The upper trace shows the variation of the separatrix elongation (dashed line), due to the departure of the TRI-IN control parameter from its reference, shown in the second row. The vertical movement was closed-loop unstable at the start of the simulation, due to the higher instability growth rate at the higher elongation. As the elongation returned to its nominal value, the vertical oscillations were stabilised. At 0.3sec, the stimulation of the coils started, indicated by the dashed line. The right hand column, using the improved initialisation procedure, illustrates acceptable behaviour.

Average flux consumption: Figure 3 (left) shows a simulation of a single limited plasma case with up-down symmetric stimulation of the E-coils, illustrating the evolution of two PF coil currents, two poloidal field probes and two flux loops. During our first attempted simulations, it was extremely difficult to match the total poloidal flux consumption between DINA and TCV. Simply matching the toroidal plasma resistance at the start of the simulation to the average toroidal resistance during the TCV discharge was inadequate. This mismatch is due to the fact that the DINA code had the transport modelling turned off and the plasma resistance was not allowed to evolve. To compensate this simplification, we added a loose feedback loop to the plasma resistance in DINA, to force a correspondence with the poloidal flux consumption. With this feedback in place, the total flux evolution shown by the evolution of the OH1 currents matches well and the fast time scale variations are unchanged, confirmed by comparison with the initial unmodified runs. Adjustment of the simulations including transport would be possible by trial and error, but nothing would be gained. The reason for the varying plasma resistance was certainly the slow evolution of plasma density and plasma impurity levels, not modelled in the simulation. Using this procedure, discharges separated by more than 2000 machine cycles could be handled without manual adjustment of the run parameters.

Drifts: Figure 3 (left) also shows a slow deviation between the simulation and experiment, which appears as an offset and a ramp in the simulation-experiment differences. One reason for this lies in the fact that the integral feedback gain only constrains the 5 control parameters at this low frequency and that, given 18 control coils, 13 degrees of freedom remain relatively unconstrained against these drifts. The drifts are induced in the controlled and uncontrolled parameters due to electronic offsets, causing integrator drift. This is due to the fact that the flux and field measurements are obtained from measured voltages which represent flux and field time derivatives. Comparing fluxes and fields therefore requires integration, which introduces a zero frequency error, namely an offset, since we inspect the traces from a time after the integrator opens, plus a drift, since a drift is the response of a perfect integrator to any constant input error. The difference between the responses at this low frequency does not concern us, since it is a

much lower frequency than the dynamic control response. We therefore remove any offset or drift in the experimental and in the simulated signals separately when presenting data in most of the figures which follow, a procedure referred to as “detrending”. The result of this low-pass filtering is illustrated in the right-hand side of Fig.3, in which the differences between the simulation and experiment at finite frequency are more clearly shown, revealing that DINA reproduces the TCV evolution in fine detail. We note that the detrending operation is applied to all measured data. The control parameter estimators, being linear combinations of these measured data, are then already automatically detrended as well. An effective bandwidth of the filtering applied by detrending is the inverse of the pulse length, corresponding to an extremely low frequency error, less than 0.1Hz. The detrending procedure does not, therefore, pollute either the simulated or experimentally measured data, but provides a simple means of separating out the finite frequency effects which concern us.

2.2 Limited discharges in the current flat top

In the earliest set of experiments [1], limited centred and up-down symmetric discharges were subjected to a complete set of PF coil square-wave voltage perturbations. These perturbations were chosen themselves to be centred and up-down asymmetric (in which case no poloidal flux change is induced for the up-down symmetric centred plasma) or up-down symmetric (in order to drive a response which drives a change in the poloidal flux, inducing radial movement and/or total plasma current modifications). Figure 4(a,b) shows a symmetric and an anti-symmetric example of the comparison between the DINA modelled responses and some experimental observations, using stimulation of the E-coils. Only a selection of experimental traces is shown, namely the 18 PF coil currents, five poloidal flux loops, five poloidal field probes and the five feedback control parameters. These two cases were chosen from the full set of five discharges, catalogued in detail in Appendix A, Figs.A.1-2 of [15]. Comparing such figures is rather subjective, but a quantitative comparison such as a mean-square difference conceals any systematic behaviour. The DINA simulations remain within the high-frequency variation of the experimental signals throughout all the simulations with the exception of slight disagreement for up-down anti-symmetric stimulation of the F1-F8 coil pair and a very low frequency difference for TRI-OUT. The low frequency differences in TRI-OUT are attributable to sight evolution of the discharge and the important observation is that no response to the particular stimulation is seen in either the experimental data or the simulation. It is difficult to hope for more and we therefore consider this agreement to be excellent.

2.3 Diverted discharges in the plasma current flat top

The next test was to compare diverted discharges which were not centred in the vessel. A complete set of such experiments was not performed, since up-down symmetric stimulations already move the eccentric plasma vertically. Fig.5 shows the flat top part of the discharge in which four of the E-coils are stimulated one at a time. The similar cases with stimulation of four

of the F-coils and both OH-coils are shown in Appendix A Fig.A.3 of [15]. In these discharges, the feedback control was removed from the 2nd and 3rd control parameters, TRI-IN and TRI-OUT, and the good agreement confirms that the control parameters are not artificially in agreement via the dominant action of the feedback loop. As in the case of the limited plasmas, the DINA simulations remain within the high-frequency variation of the experimental signals throughout almost all the simulations and we therefore again consider this agreement to be excellent. The only small but systematic disagreement was observed for the response to the OH1 and OH2 stimulation.

The square pulse voltage stimulation of the OH1 and OH2 coils led to vertical position oscillations during the resulting excursions. These oscillations had been seen in previous work and a non-linear evolution of the plasma response had been suggested as the most likely explanation [2]. Figure 6 shows an expanded view of the response to the OH1 square voltage pulse. The oscillations in the vertical position are well reproduced by the DINA simulation. The envelope increases around 400msec, showing that the closed loop of TCV has gone unstable, with a growth time in the range 200-400msec. After 100msec, the oscillations are damped, showing that the closed loop has become stable again. This change in closed loop stability is attributable to the transient increase in the vertical field decay index which causes an excursion of the plasma elongation. The closed loop is unstable during the increase in elongation from 1.45 to 1.53. This observation is an example of non-time-invariant behaviour in the experiment and the simulation, unlike the responses seen previously. This behaviour can never be simulated by any of the linearised models, for which the assumption of time invariance is intrinsic.

2.4 Full scenario including the limited-diverted transition

We next performed a full scenario simulation of TCV discharge #12610. The flat top equilibrium was diverted and the separatrix is illustrated in Fig.1. The scenario was as follows. The simulation was launched at the first reconstructed equilibrium with only 50kA of plasma current. The simulation continued up until 970ms, at which time the plasma current had returned to 38kA. The plasma diverted at 308msec and became limited again at 834msec. The square pulse voltage stimulation was applied to coils OH1 and OH2. Figure 7(a) compares the same set of selected electromagnetic parameters as used in Figs. 4(a), 4(b) and 5. Figure 7(b) compares some geometrical parameters. No detrending is applied to these results, since we are no longer considering small variations around a nominal operating point. Figures 7(a,b) show no evidence of any discontinuity in the agreement between DINA and the TCV observations during the limited-diverted transitions in either direction. The agreement between all signals in Fig. 7(a) is satisfying, with the exception of TRI-IN and TRI-OUT. These two parameters were not feedback controlled in this discharge, as mentioned in section 2.3. The simulation and discharge signals drift apart linearly, illustrating the argument on drifts in section 2.1.

The DINA simulations contain a simple Kadomtsev-like sawtooth model which causes a redistribution of the plasma core when q(0) drops below 0.9. The value of the safety factor then

decreases again, as the core re-heats and the poloidal flux diffuses, provoking a sawtooth cycle. Figure 8 illustrates the evolution of the plasma current, the central safety factor and the sawteeth in both the DINA simulation and in TCV. No central safety factor measurement is available on TCV but the sawtooth onset can be deduced from a soft X-ray signal viewing the centre of the plasma (centre row). Two differences are obvious between the simulation and the experiment. Firstly, the sawtooth period is much longer in the solid line simulation, (shown in the right hand column with the expanded time scale). The sawtooth frequency of the simple model in the simulations increases with an increase in the q(0) threshold assumed for the crash, which has a somewhat arbitrarily chosen value. More importantly, the onset of the sawtooth activity occurs much earlier during the full plasma discharge in TCV than in the DINA simulation. The total toroidal plasma resistance in the simulation has been adjusted to fit the experimental values and provides the dissipation to allow normal poloidal flux diffusion. An earlier onset implies that the penetration of the poloidal flux is significantly faster than the toroidal resistance should allow. The flux penetration time is sensitive to the assumed temperature profiles so this full discharge simulation was repeated with more peaked (narrow) and less peaked (wide) electron temperature profiles. In addition, the transport (assumed to follow ITER-89 L-mode scaling) was enabled for a third additional case. The lower row in Fig.8 shows that the wide temperature profile (dotted line) which corresponds to a very low value of the internal inductance, li ~ 0.6 at t=0.2sec, never allows q(0) to drop below 1.4 and can be excluded. The narrow temperature profile (dashed line) reaches q=1.0 at t=0.25sec but has a higher internal inductance, li~1.2. Enabling heat transport in the simulation (dotted-dashed line) led to an even earlier crossing of q(0)=1 in the simulation, at t=0.20. The reconstructed equilibrium had li~0.9 at this time, similar to the standard DINA simulation (solid line). We conclude that extreme profile changes and enabling transport do not reduce the sawtooth onset time to its experimentally determined value at t=0.16sec and that the lowest sawtooth onset times are obtained with values of internal inductance much higher than that obtained from reconstruction of the equilibrium. The hypothesis of enhanced transport of the poloidal flux during the plasma current ramp-up is therefore justified. The bottom right panel of Fig.8 shows a faster sawtooth period obtained with the narrow electron temperature profile, much closer to the experimentally observed value, again illustrating a sensitivity of the model to the assumed profiles.

3 COMPARISON IN THE FREQUENCY DOMAIN

A series of experiments on TCV demonstrated the practicality of measuring the unstable open-loop model by using multiple frequency stimulation [3, 16]. The same technique was applied to the DINA code by simulating the same 18 TCV shots, which stimulated all 18 external PF coils. This complements the time domain analysis of the DINA TCV model.

We have found that the previous approach [3] did not maximise the information about differences between the various models. In that work, the transfer function was estimated from the voltage input into the coil power supplies. More sensitive information may be gained by considering directly the voltage applied to the PF coils as the plant input, Fig.9. This difference is due to the

presence of weak proportional gain in the power supply current control feedback loop, which makes the PF coils appear much more resistive than their physical resistance. This effective resistance introduces a roll-off of the transfer function at frequencies where the real TCV PF coils behave as integrators. Figure 10 illustrates how the inclusion of a power supply model can act to mask model differences in the transfer function. This figure shows the response of a sixth parameter, PSI-R to voltages applied to PF coil F7. This parameter estimates the radial movement but was not used in the feedback control loop. The Bode plots on the right show the complex response of PSI-R to the voltage on the coil F7 while the Bode plots on the left show the response to the voltage applied to the F7 power supply. Discrimination between the model predictions is clearly seen in the former and hidden in the latter. All the frequency analysis in the present paper uses the actual coil voltages rather than the power supply demand signal. The associated cost with this approach is a worse signal to noise ratio due to the thyristor switching in the power supplies at a frequency around 600Hz which was the original reason for using the power supply inputs as data.

We briefly recall the analysis method used in the original work [3]. Multi-sine voltage perturbations were applied to the PF coils during the plasma current flat top, spanning the frequency range of 20-3000 rad/s. The voltage input stimulation was $V_{in} = \sum_{n=1}^{29} a_n \sin(\omega_n t + \Phi_n)$, and the phases φ_n were chosen to minimise the maximum amplitude of V_{in}. The amplitude vector α_n was boosted at high frequencies in order to overcome the expected plant attenuation. 18 independent experiments were performed to identify the transfer functions for the 18 PF coil voltages.

The frequency response of TCV was calculated using the following procedure. For each of the 18 experiments we evaluated the magnitude and phase response of all the input and output signals at the frequency components of our stimulation signal. For a given experiment, at each frequency ω_n, we may define $\mathbf{y}(\omega_n)$ as the column vector of the output responses, $\mathbf{u}(\omega_n)$ as the column vector of the input responses and $\mathbf{G}(\omega_n)$ as the frequency response of TCV, such that $\mathbf{y}(\omega_n)=\mathbf{G}(\omega_n)\mathbf{u}(\omega_n)$. $\mathbf{y}(\omega_n)$ contains the 5 control parameter responses, $\mathbf{u}(\omega_n)$ contains the 18 PF coil responses and matrix $\mathbf{G}(\omega_n)$ is therefore of rank 5x18. The **y** and **u** vectors for each of the 18 experiments are combined together to create the blocked sets of results, **Y**(5x18) and **U**(18x18). The frequency response estimate of TCV was then evaluated from $\mathbf{G}(\omega_n) = \mathbf{Y}(\omega_n) * \mathbf{U}(\omega_n)^{-1}$.

This analysis procedure was applied identically to the TCV measurements and to the DINA simulation results and a comparison is shown in Fig.11. It is interesting to compare the quality of the DINA responses with the quality of the responses of linear models, namely with the CREATE-L model [17] derived from a deformable plasma equilibrium and the RZIP model [18] derived from the assumption of radial and vertical displacement of a fixed plasma current distribution shape. In Fig.11, the identified frequency responses of TCV and DINA are compared with these two linear models. There are 216 responses to be compared and we only show a representative set spanning the three coil types and three of the control parameters.

The top row is typical of about 75% of the data, all of the models and the experimental data show agreement within the dispersion of the data. The remaining results have either one (second row of the figure) or both (bottom row of the figure) of the linear models showing systematic disagreement with the data. For all of the data, the DINA model and the experimental data are in agreement within the dispersion, allowing us to conclude that the physical model of TCV used in DINA is adequate for simulating the equilibrium plasma response of TCV.

4 DIFFERENCES BETWEEN LINEAR AND NON-LINEAR MODELS

It is interesting to compare the quality of the DINA time domain responses with the quality of the equivalent responses of the linear models to these control system stimulations. Since the responses of the linear models were already accurate, it is not surprising that the non-linear DINA modelling is also accurate. It is only any differences between the experimental results and the predictions of the linear models which justify recourse to a more complicated and time-consuming non-linear model. Some differences in the time domain response to the square voltage pulse simulation were noticed when comparing TCV with linear models, even if for only very few input-output transfer functions. The full set of comparisons is shown in Appendix A Fig.A.4 of [15]. A good example of disagreement, bearing in mind that most of the cases show perfect agreement, is the response to up-down symmetric excitation of the E-coils, shown in Fig.12. The DINA and simulations of the linear models overlap for all the TRI-OUT and Ip responses and the zIp response is minimal by design. However, the TRI-IN response is less well simulated by the RZIP model for one coil pair and the fast radial movement (P-VERT) is less well simulated by RZIP than by CREATE-L. This last case is actually better simulated by CREATE-L than DINA. However, several CREATE-L assumptions had been tested to obtain this excellent agreement, whereas the DINA simulations were not iterated to obtain the agreement documented in this paper.

5 DISCUSSION AND CONCLUSION

The DINA code was successfully implemented to simulate the closed loop operation of the TCV tokamak for modest growth rate vertically unstable plasmas. Three sets of previous experiments were simulated with recourse to trial and error optimisation and the comparison with these extensive TCV results is extremely encouraging. Limited and diverted plasmas showed no discrepancy in the time domain or in the frequency domain plasma equilibrium responses, supporting the assumption that the DINA model is an excellent platform for developing and testing feedback controllers for present and future devices. During these simulations non-linear behaviour due to the excursion of the equilibrium from the initial equilibrium were identified and correctly simulated by the DINA code. Such behaviour is excluded from studies using linear tokamak models. The previous frequency domain analysis was extended to consider the PF coil voltages, showing that the model discrimination is improved, even if the signal to noise in the transfer function estimates has worsened.

The only significant disagreement between DINA and TCV concerned the onset of the sawtoothing activity which occurs earlier in the experiment than in the simulation in spite of adjustment of the toroidal loop resistance during the simulation and even considering abnormally narrow temperature profiles. This suggests that the poloidal flux diffuses inwards on a time scale which is faster than that determined by the toroidal plasma resistance and care should be taken in simulating the evolution of the safety factor profile until this difference is understood.

Although simulations of the full tokamak feedback control system have already been presented in [7], this work extends those results by the completeness of the stimulation, using all PF coils of a flexibly shaped tokamak and by covering both limited and diverted plasmas. Our confidence in the quantitative precision of the DINA simulations has been enhanced by extending our analysis into the frequency domain, showing that the physics included in the DINA code is adequate for modelling the plasma equilibrium response at the driven frequencies.

The differences between the DINA simulations and TCV are sometimes smaller than the already acceptably small differences between the TCV experimental results and the linearised model simulations. Future work will concentrate on higher growth rate TCV discharges, comparing the growth rates measured on DINA simulations with those measured experimentally, as well as attending to the small number of identified linear model differences and the question of current profile penetration.

ACKNOWLEDGEMENTS

Benchmarking these TCV experiments against the DINA code was first suggested at an ITER Expert Group meeting on MHD, Control and Disruptions. Thanks go to the TCV team without whom the experimental results would not be comparable with the model and to A.S. Sharma and Prof. D.J.N. Limebeer for useful discussions on the modelling. Two of the authors (RK, VL) thank the CRPP for their hospitality during visits to Lausanne. This work was partly supported by the Swiss National Science Foundation**.** One of the authors (JPW) was partly supported by the United Kingdom EPSRC.

REFERENCES

[1] Villone F., Vyas P., Lister J.B., Albanese R., Nuclear Fusion **37** (1997) 1395
[2] Vyas P., Villone F., Lister J.B., Albanese R., Nuclear Fusion **38** (1998) 1043
[3] Coutlis A. et al., Nuclear Fusion **39** (1999) 663
[4] Khayrutdinov R.R., and Lukash V.E., J. Comp. Physics **109** (1993) 193
[5] Lister J.B. et al., Fusion Technology **32** (1997) 321
[6] Hofmann F. et al., Nuclear Fusion **38** (1998) 399
[7] Humphreys D.A., Khayrutdinov R.R., Lukash V.E., Bull. APS **40** (1995) 1191
[8] Vasiliev N.N., Khayrutdinov R.R., Lukash V.E., et al., Preprint IAE-6074/7, Moscow

[9] Mondino P.L. et al., 20th SOFT, Marseille, France, 1998, Vol.1, p. 595
[10] Humphreys D.A., Khayrutdinov R.R., Lukash V.E., et al., Bull. APS **39** (1994) 1650
[11] Khayrutdinov R.R., Yoshino R. et al., “Plasma Equilibrium at VDE with a Halo Current Spike in JT-60U”, to be submitted to Nuclear Fusion
[12] Lukash V.E., and Khayrutdinov R.R., Plasma Physics Reports **22** (1996) 99
[13] Hofmann F. and Tonetti G., Nuclear Fusion **28** (1988) 1871
[14] Hofmann F. et al., Nuclear Fusion **37** (1997) 681
[15] Khayrutdinov R.R., Lister J.B., Lukash V.E., Wainwright J.P. "Comparing DINA code simulations with TCV experimental plasma equilibrium responses", LRP 673/00 (2000)
[16] Wainwright J.P. et al., IEEE Transactions on Control Systems Technology **7** (2000) in press.
[17] Albanese R., Villone F., Nuclear Fusion **38** (1998) 723
[18] Lister J.B., Sharma A.S., Limebeer D.J.N., Nakamura Y., Wainwright J.P., Yoshino R., "Plasma equilibrium response of Ohmically and NBI heated discharges in JT-60U", LRP 680/00, see also [3]

FIGURES

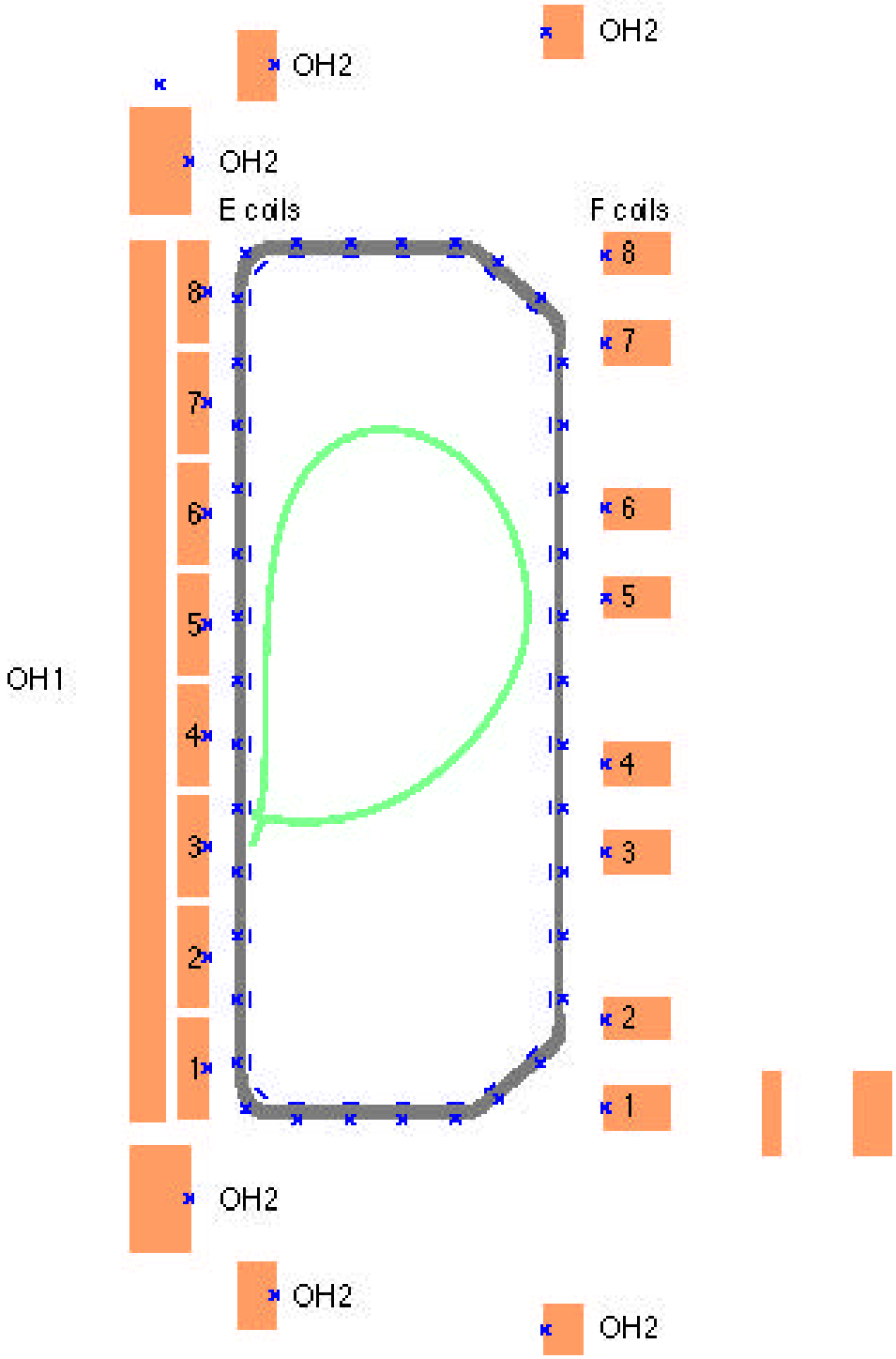

Fig.1 The TCV vacuum vessel, PF coils, poloidal field probes (marked '-' inside the tiles) and flux loops (marked 'x'). The last closed flux surface contour is the nominal single null diverted plasma, pulse #12610.

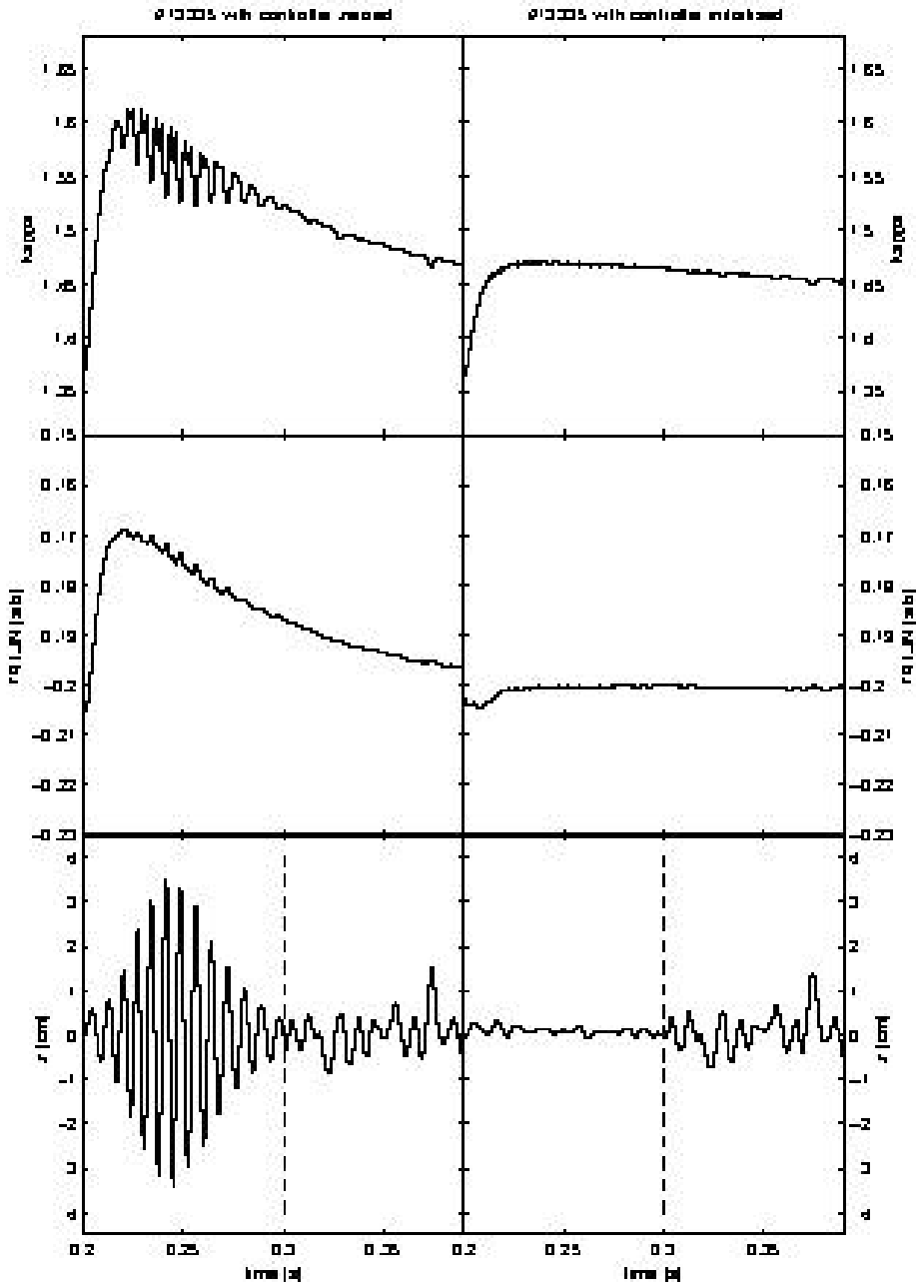

Fig.2 Improvement to the controller initialisation caused a significant reduction to the transients at the start of the DINA simulation (right). Uninitialised (left), the transient induced an increase to the vertical field decay index and hence to the elongation (top trace), resulting in an anomalous vertical instability showing up on the vertical movement trace (bottom) which caused a failure of the simulation in early tests. The middle trace shows the excursion of the control parameter for elongation. The start of the stimulation is indicated as a vertical dashed line.

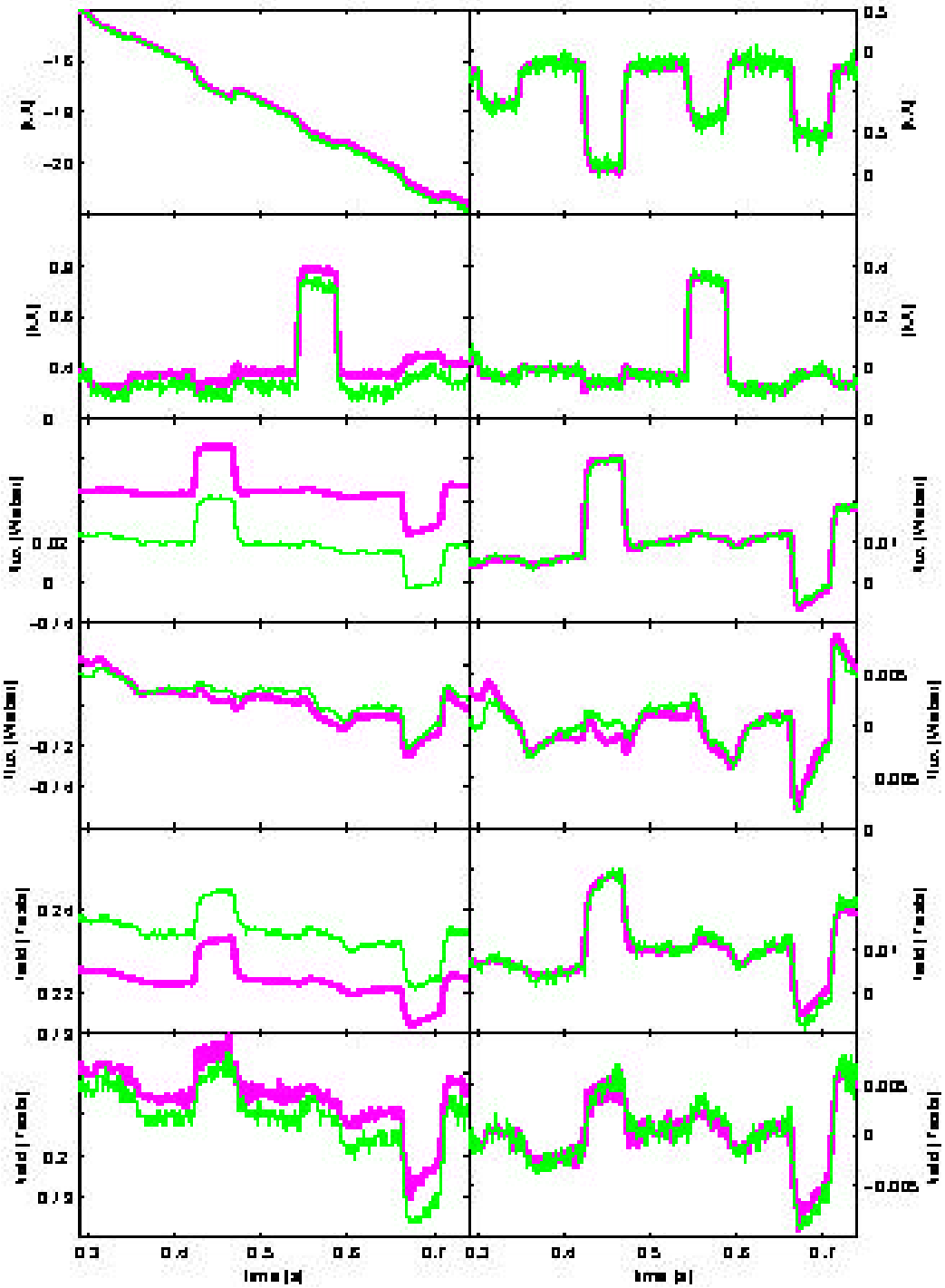

Fig.3 Simulation of a TCV plasma response experiment (thin green line) with the DINA code (thick red line), with loose flux consumption feedback, illustrating (left) low frequency drifts; (right) the same responses with the slow variation filtered, referred to as detrended. From top to bottom the signals in both columns represent: PF current OH1, PF current E2, flux loops #3 and #13, poloidal field probes #3 and #13.

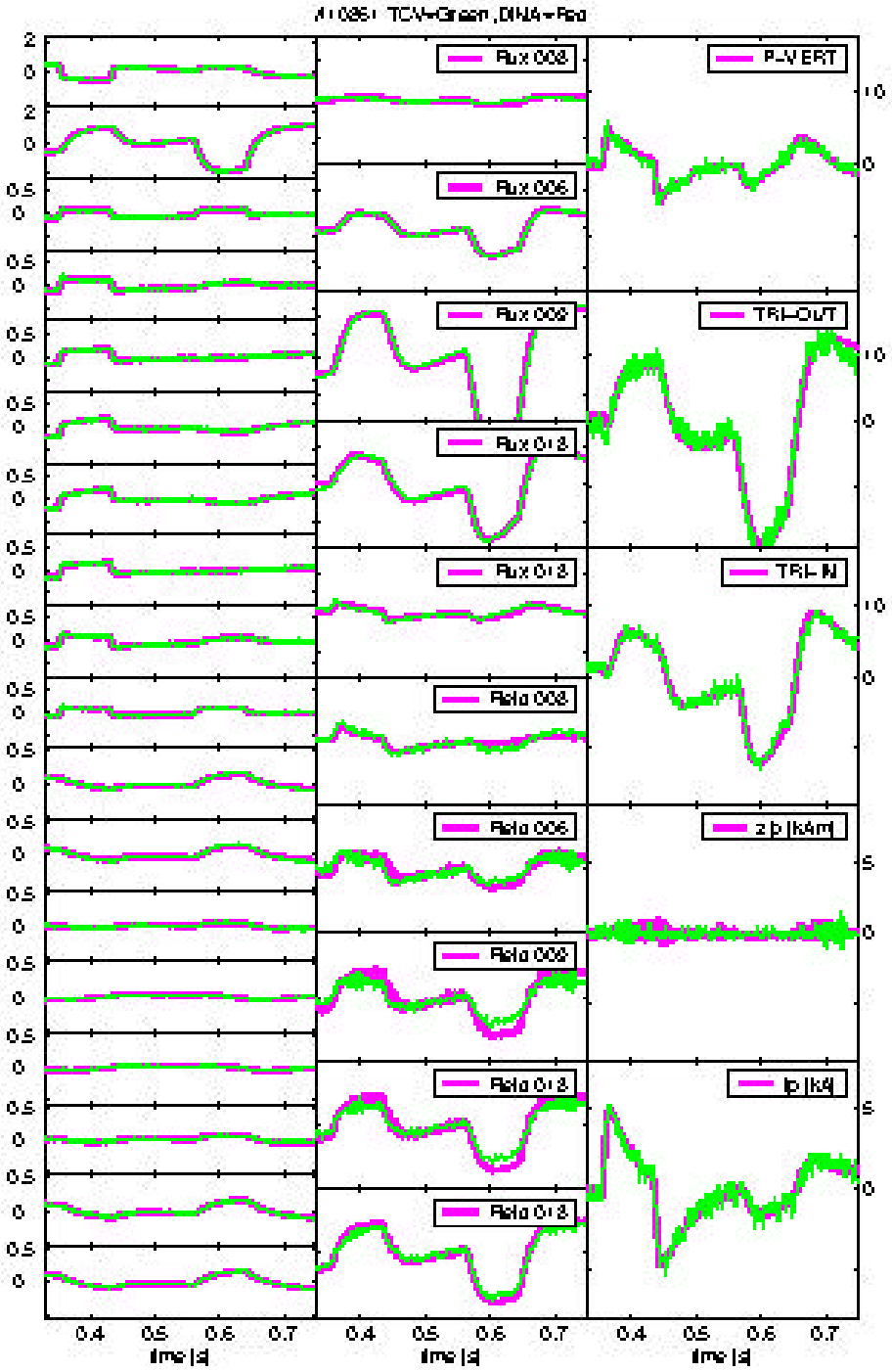

Fig.4a) Comparison between the experimental response (noisier green lines) and the DINA response (red lines) for excitation of the OH-coils. The signals are shown detrended: (left column) all 18 external PF coil currents, OH1, OH2, E1 to E8, F1 to F8; (middle column) flux loops #3,6,9,13,18, magnetic probes #3,6,9,13,18; (right column) the five feedback control parameters.

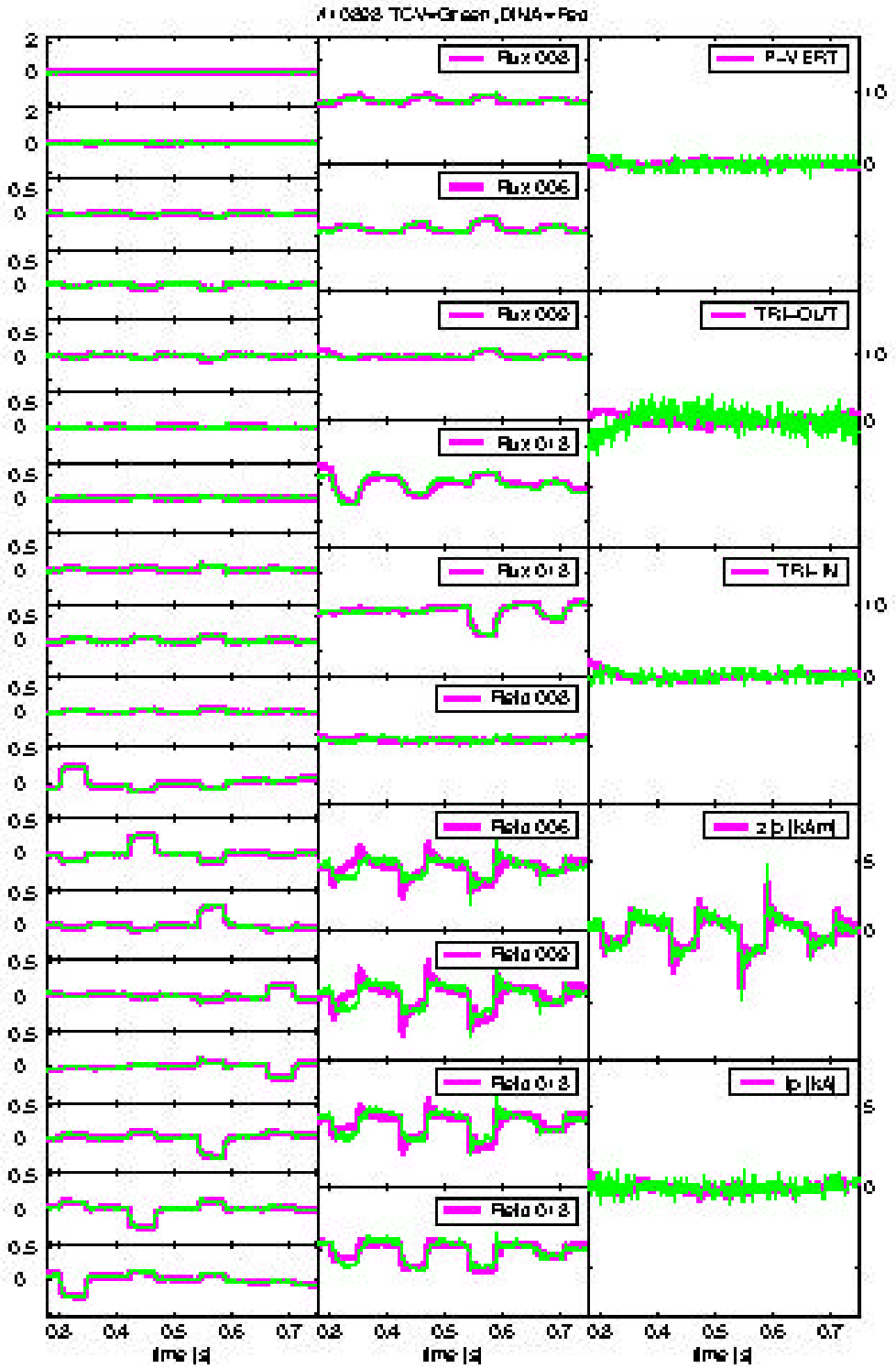

Fig.4b) Comparison between the experimental response (noisier greenline) and the DINA response (red line) for up-down anti-symmetric excitation of the F-coils. The signals are as in Fig. 4a).

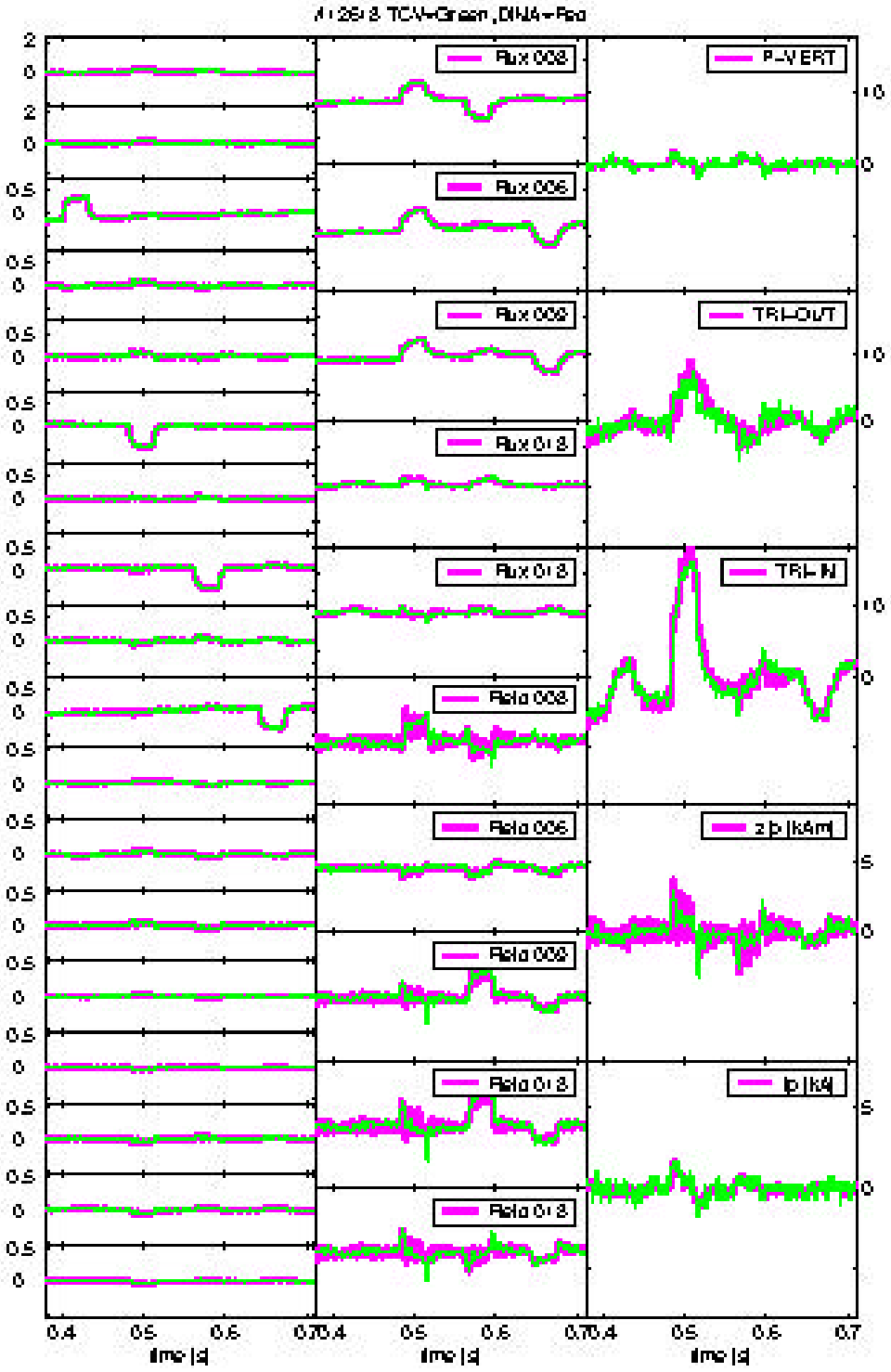

Fig.5 Simulation of a diverted off-centred plasma, using separate E1, E4, E6, E8 coil stimulations in a single pulse. Signals are as in Fig.4a).

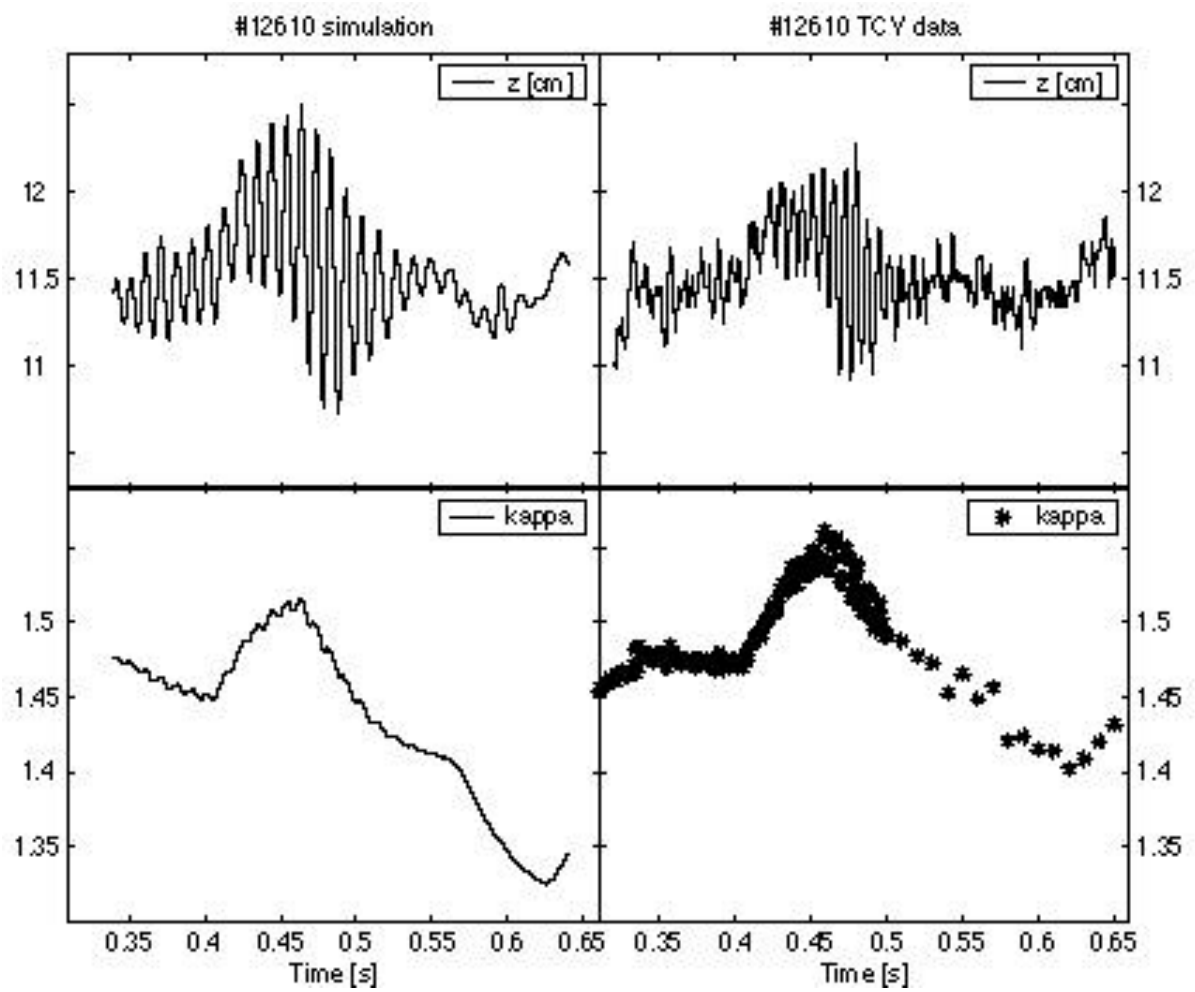

Fig.6 Comparison between TCV (left) and the DINA simulation (right) for a large excursion due to a square voltage pulse OH1 stimulation. The vertical position goes closed loop unstable and returns to closed loop stable once the elongation is reduced.

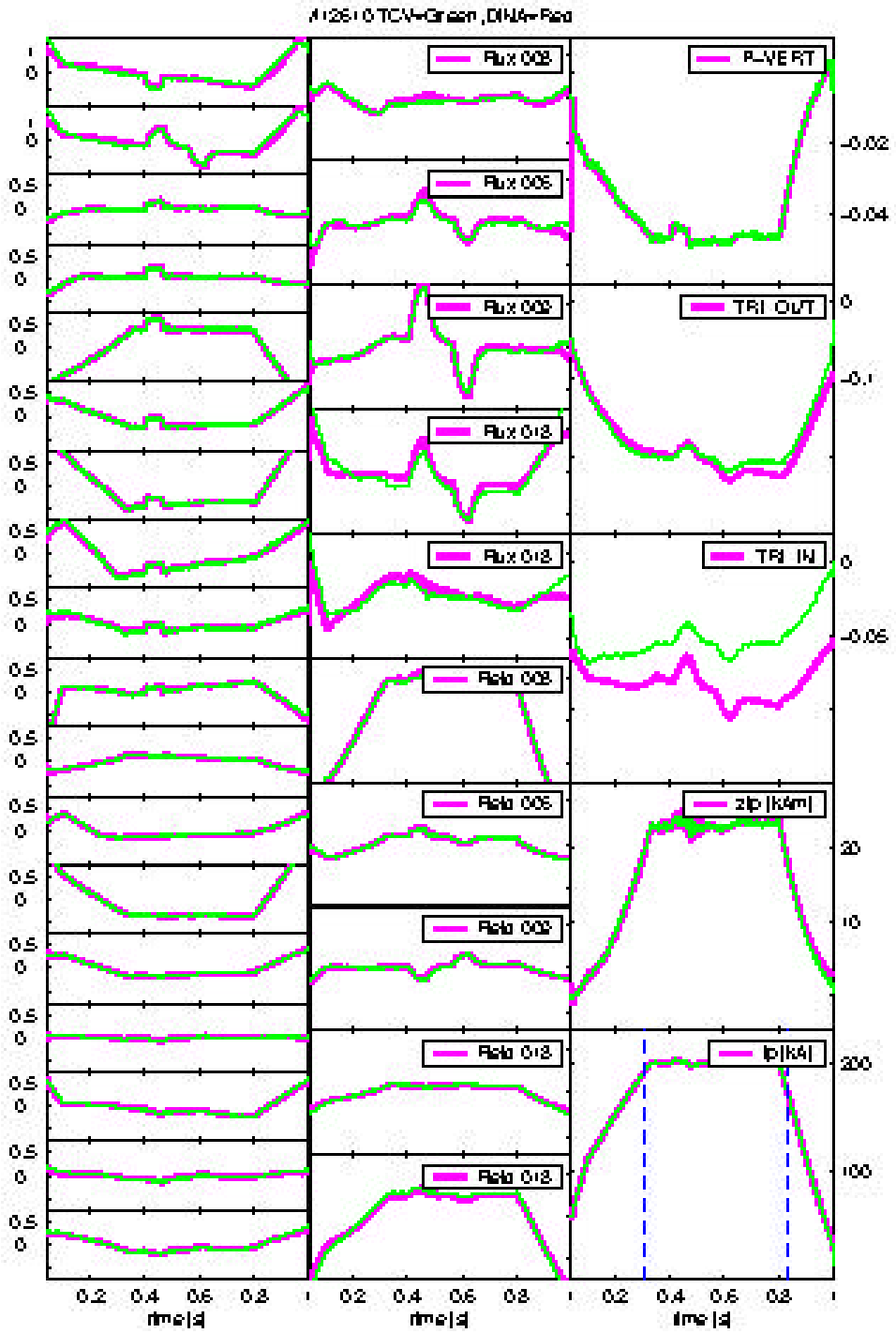

Fig.7a) Simulation of a diverted off-centred plasma, using OH1 and OH2 coil stimulations in a single pulse. The plasma diverts at 308 msec and becomes limited again at 834 msec, shown as vertical dotted lines. a) Electromagnetic parameters as in Fig.4a). Control parameters TRI-IN and TRI-OUT were not fedback during the discharge, explaining the linear drifting apart since the signals are not detrended.

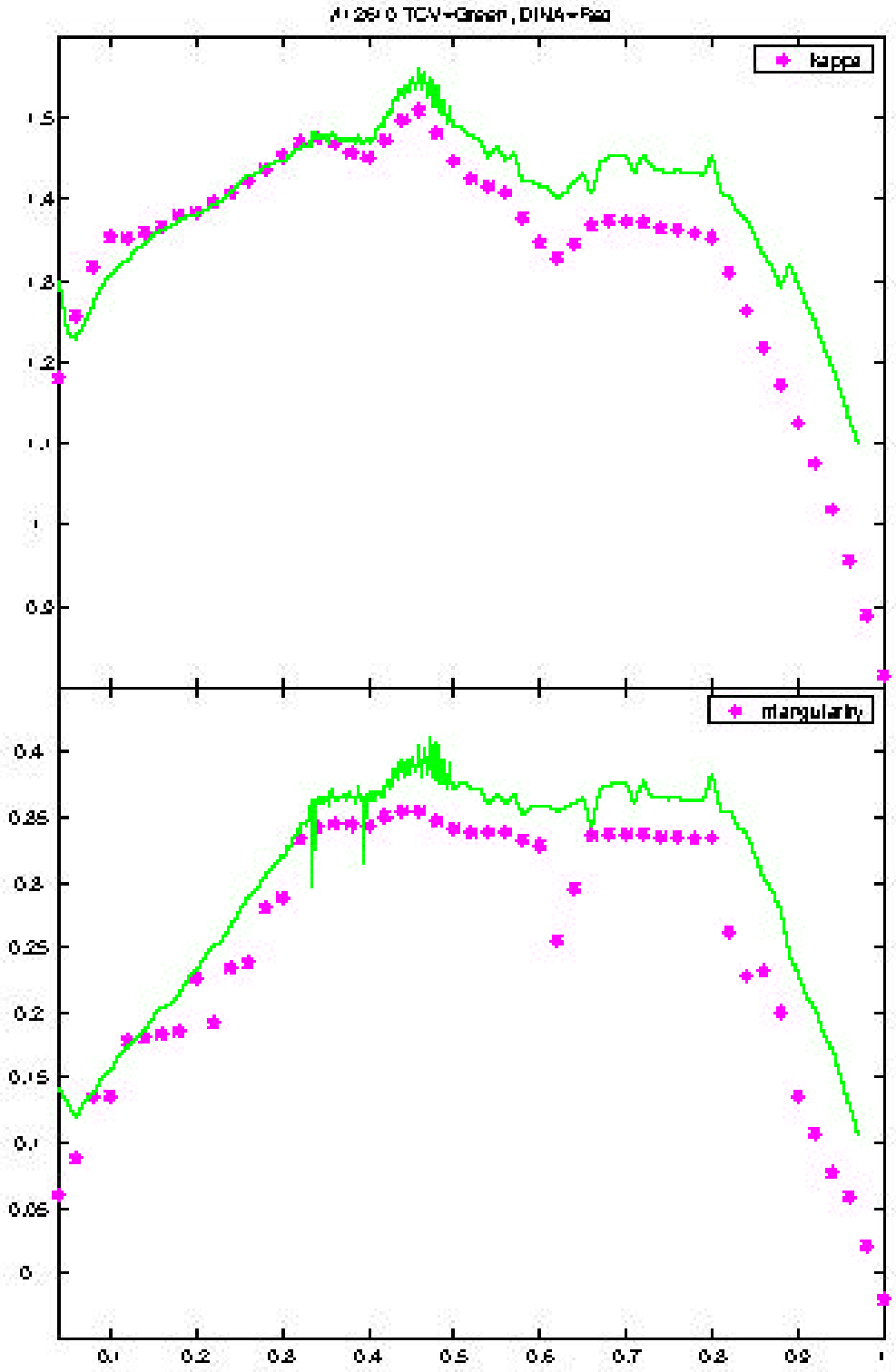

Fig.7(b) Comparisons of elongation and triangularity during the full discharge simulation. The solid line is the TCV reconstructed data and the points are the DINA simulation.

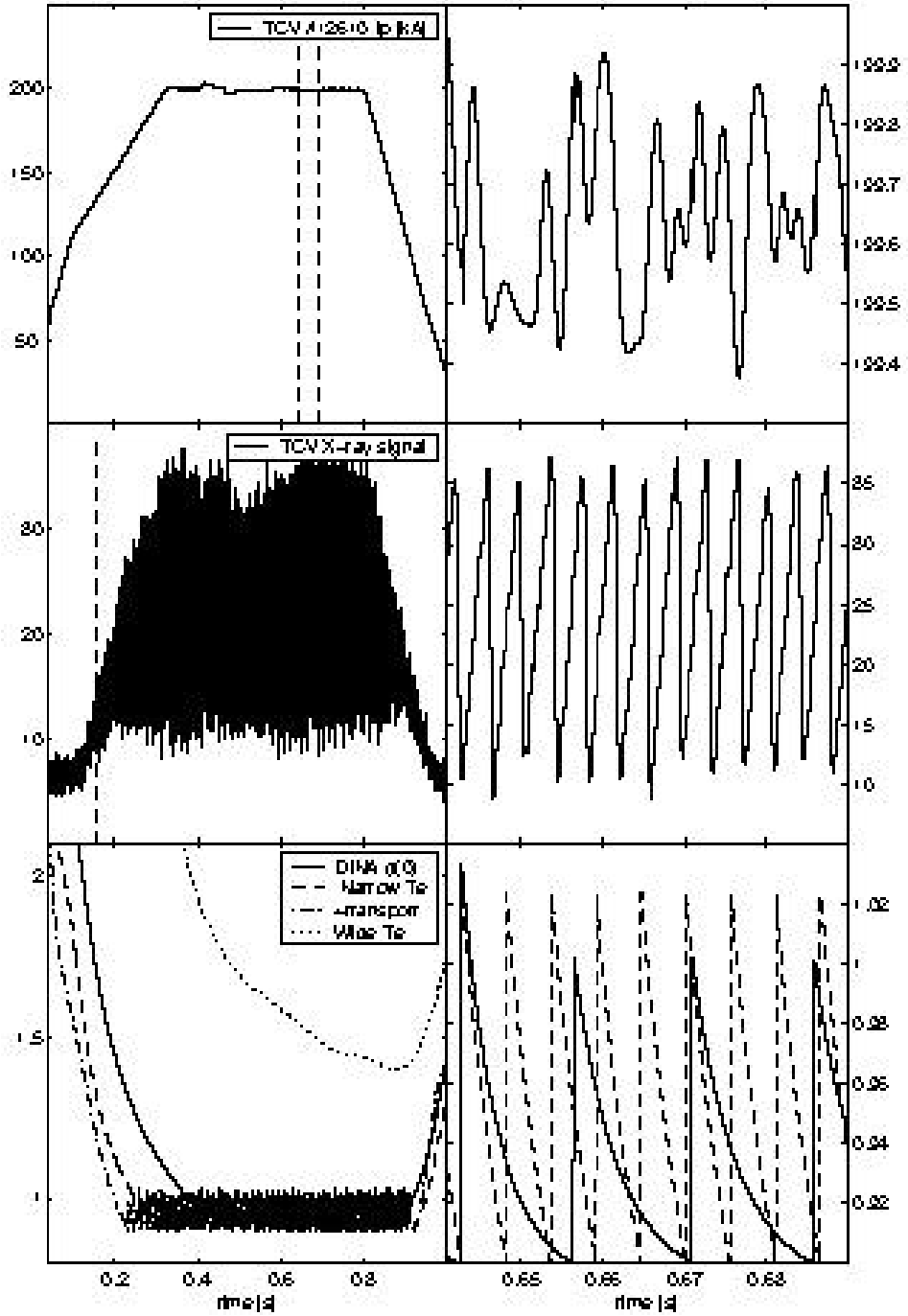

Fig.8 Comparison between DINA simulation and TCV for the evolution of the sawtooth activity: left, the full pulse showing, from top to bottom: TCV Ip, TCV soft X-ray signal, DINA q(0); right, an expanded view of the same signals between the dashed vertical lines on the left. The simulations were repeated for different assumed profiles, shown in the lower row.

Title: Micrografx Designer 6.0 - tcv closed loop.dsf
Creator: Adobe Printer Driver 3.0 for Windows 3.1
CreationDate: 02/24/97 11:43:37

Fig.9 Schematic diagram of the TCV control system, illustrating the difference between considering the power supply demand voltage and considering the PF coil voltage as the system input, in the presence of proportional current control in the power supply.

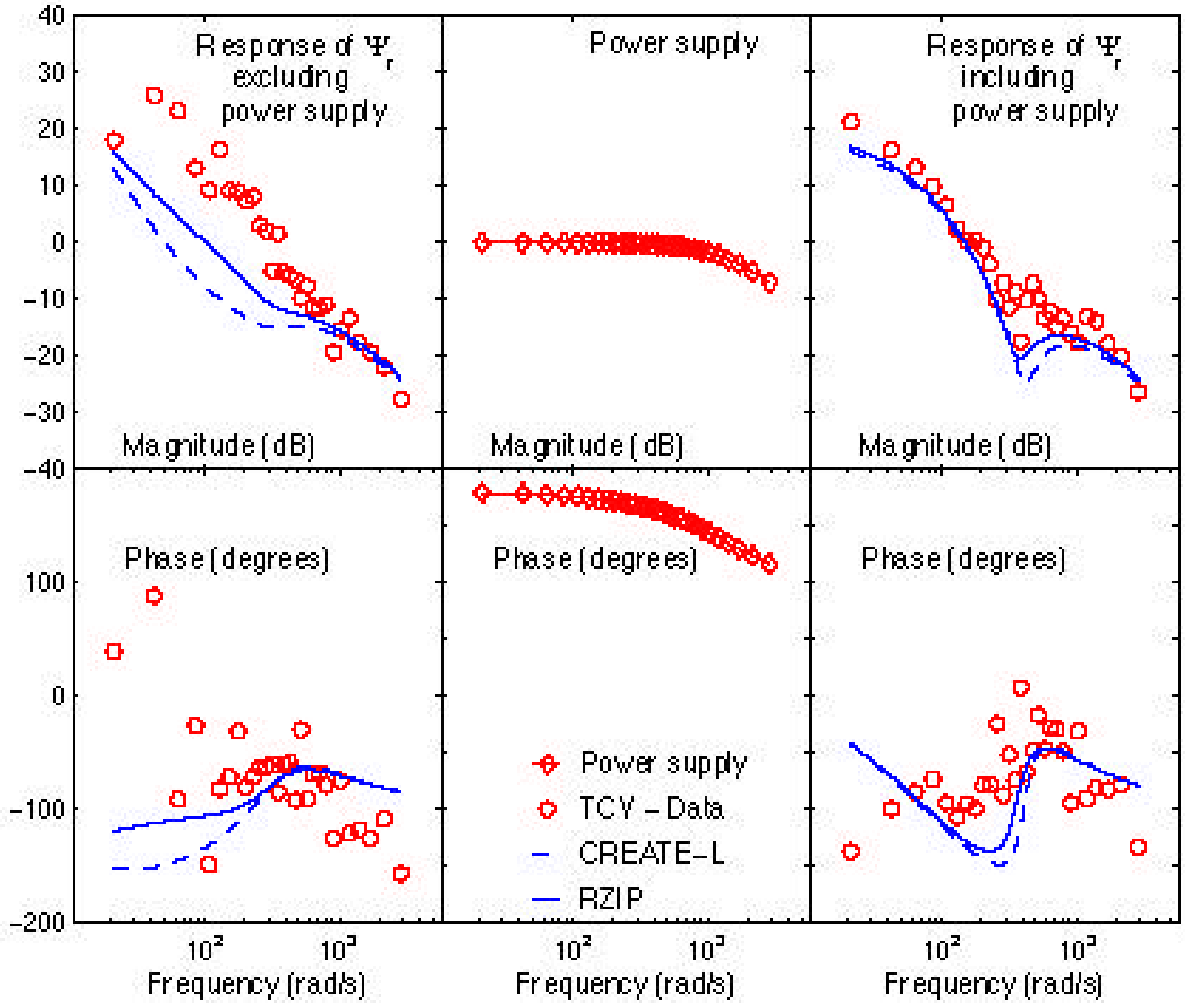

Fig.10 This figure illustrates the masking effect of the coil power supply model on the data. The left hand Bode plots show the response of the control parameter to voltages applied to directly to PF coil F7. The red circles are the experimental data, the dashed blue line is the prediction of the CREATE-L model, the solid blue line is the prediction of the RZIP model. The middle column shows the power supply model for coil F7 (points and curves) while the right hand column shows the data and modelled responses at the input to the F7 power supply.

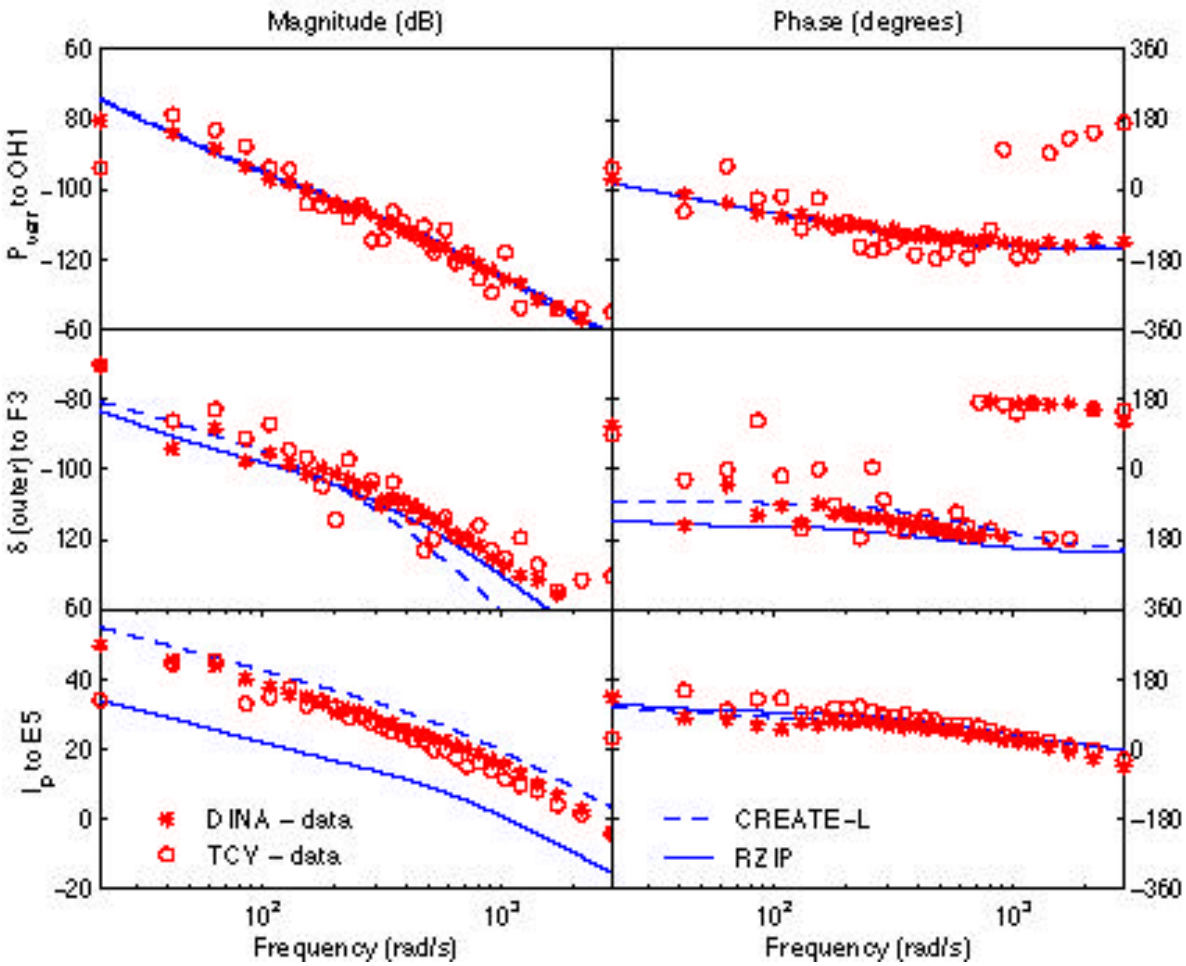

Fig.11 Excellent agreement between the DINA simulations and the TCV experimental data. RZIP and CREATE-L linear models are included for comparison. The phase is indicated between -180 and 180 degrees, causing apparent jumps at the extremes of this range.

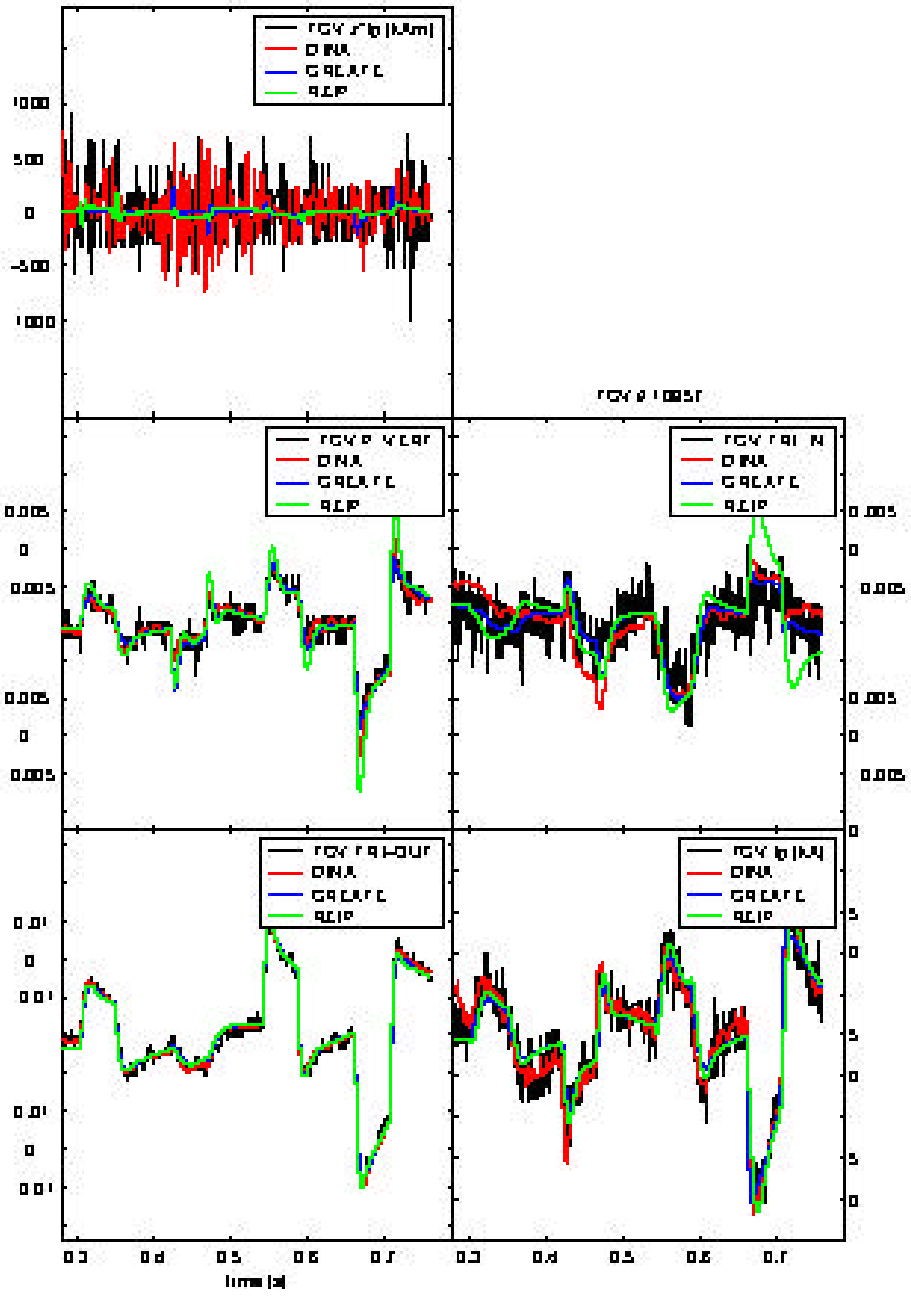

Fig.12 Expanded view of the response to up-down symmetric stimulation, showing differences between the DINA simulation , the TCV observations and the two linearised models RZIP and CREATE-L.